Journal of Electroanalytical Chemistry 977 (2025) 118829

Contents lists available at ScienceDirect

Journal of Electroanalytical Chemistry

journal homepage: www.elsevier.com/locate/jelechem

Novel autocalibration strategy for disposable potentiometric test strips

Antonio Calvo-López, Laia Garrido-Carretero, Julián Alonso-Chamarro, Mar Puyol *

Group of Sensors and Biosensors, Department of Chemistry, Autonomous University of Barcelona, Edifici Cn, 08193 Barcelona, Spain

ARTICLE INFO

Keywords:
Autocalibration
Potentiometry
Ion selective electrodes
Disposable test strips
Chloride ion
Sweat
Cystic fibrosis

ABSTRACT

Potentiometry, particularly involving ion-selective electrodes (ISEs), is widely employed in laboratories due to its selectivity and compatibility with portable instruments. However, ISEs face a drawback —instability over time, requiring frequent calibration for precise and reliable results. This manual calibration process contradicts the user-friendly concept and inhibits the development of single-use quantitative devices for untrained personnel. To solve this limitation, a novel potentiometric autocalibration procedure, which is automated, is presented, and successfully tested for the first time with versatile potentiometric disposable test strips to perform the determination of chloride ion in sweat as a demonstrator. The test strips are based on a cyclic olefin copolymer platform, where two identical Ag/AgCl chloride ISEs are integrated, one acting as indicator and the other as reference electrode. Comparison of chloride results in real sweat samples between those obtained with the proposed test strips performing the novel autocalibration procedure and using ion chromatography reveals that the automated procedure effectively allows quantitative chloride ion analysis with good analytical features: linear range from 10 to 150 mM (covering the pathological range), average inter-method error of 7 % and average RSD between test strips of 4 %. By carefully selecting the initial solution composition in direct contact with each electrode, the autocalibration ensures that potentiometric test strips can be calibrated just before its use without requiring conscious user involvement. This breakthrough not only streamlines the process but also opens the possibility for the development of cheap disposable potentiometric test strips, accessible to non-experts operators, to quantitatively determine selected analytes in different fields.

1. Introduction

Nowadays, one of the most important challenges in the area of analytical chemistry focuses on solving the need for miniaturized, low-cost and easy-to-use analytical instrumentation, which allows obtaining, in real time and in situ, useful analytical information about specific (bio)chemical compounds at increasingly low concentrations and small sample volumes with extremely complex matrices [1,2]. These demands stimulate the development of novel analytical methodologies such those based on (bio)chemical sensors in which sample pretreatment is drastically reduced thanks to its selectivity. Lately, great advances in this area have been done by combining (bio)chemical sensors and microfluidics for the development of miniaturized analytical instrumentation, arising the Lab-on-a-chip (LoC) concept [3,4]. These miniaturized devices are capable to fulfill most of the necessary analytical quality features of analytical instrumentation. In this sense, they offer portability, automation, integration of the different stages of the analytical procedure and reduced energy consumption, reagents and sample volumes, wastes generation, analysis time and overall costs per analysis [5–9]. Test strips can be considered as a simplified form of LoC devices, where the principles of miniaturization and integration are applied for on-site or point-of-care analysis. While LoC devices cover a broader spectrum of complexity, ranging from simple microfluidic chips to highly sophisticated devices with integrated sensors, microvalves, and control systems, test strips focus on specific assays and are particularly well-suited for scenarios where simplicity and speed are essential [10,11].

Potentiometry emerges as an ideal quantitative detection technique for integration into microfluidic platforms or test strips, owing to its conceptual and instrumental simplicity, as well as its inherent potential for seamless automation. It is also characterized by wide linear ranges and robustness, so its applicability is wide in different fields [12–15]. Commercial potentiometric equipment consist mainly of an electrochemical cell structure, which includes two different types of electrodes: one or several Ion Selective Electrodes (ISEs) and another one acting as reference electrode [16], which can operate efficiently in both batch or flow continuous mode. Their integration into microfluidics to develop

* Corresponding author.
E-mail address: mariadelmar.puyol@uab.es (M. Puyol).

https://doi.org/10.1016/j.jelechem.2024.118829
Received 19 October 2024; Accepted 25 November 2024
Available online 1 December 2024

LoC devices has been proven to provide excellent analytical features however, in all cases they need frequent recalibration to achieve accurate and repeatable results [13–15,17]. Although different disposable potentiometric devices/test strips have been proposed, their main limitation is the inexistence of a reliable, simple and inexpensive automated calibration protocol that can be performed prior to each quantitative sample analysis and without the user intervention, making them economically and commercially viable [18–21].

The concept of symmetrical potentiometric cells was presented for non-miniaturized and intensive use systems [22,23]. In this case, two identical ion-selective electrodes are used, one acting as an indicator and the other as a reference. This allows reducing signal noise and increasing electrode stability over time, obtaining systems that do not require such frequent recalibration. In the case of disposable analytical devices, the concept of calibration-free potentiometric electrodes, similar to the amperometric glucometer, emerged as an option to consider [24–26]. In this approach, by evaluating a few test strips from an entire manufacturing batch, an initial factory calibration could be obtained. However, it is still a long way off to apply this strategy to ISEs because Nernst equation coefficients depend on many variables (test strip packaging, storage conditions, ion selective electrode conditioning and measurement conditions, among others). This fact prevents the effectiveness of a factory calibration, especially when accurate and precise quantitative results are needed, and forces a calibration to be carried out ideally just before the measurement process.

In this scenario, we propose a new autocalibration concept to be applied in quantitative potentiometric disposable test strips, which was patented in 2018 [27]. It is based on using versatile microfluidic platforms (test strips) containing an electrochemical cell integrated by two identical ISEs, thus selective to the same analyte. One of them acts as indicator electrode and the other one as reference electrode. By means of a proper selection of the composition of the solutions in contact with each electrode, it is possible to calibrate the test strip (to obtain Nernst equation coefficients – see Eq. (1) in section 2.4. *"Novel autocalibration procedure"*) just before sample analysis, under the same sample measurement conditions. With this new conceptual approach, it is guaranteed that several months after its manufacturing and packaging, the test strip can be calibrated when used without conscious user intervention, thus increasing the overall potentiometric device robustness and simplicity.

For the manufacturing of the disposable potentiometric test strips, microfabrication techniques based on polymer multilamination have been employed using cyclic olefin copolymer (COC) as polymeric substrate. It offers multiple advantages such as high mechanical and chemical resistance, high biocompatibility, low water absorption, and fairly good compatibility with conductive inks and pastes to integrate electrodes and conductive tracks for electrochemical devices [28–32].

In the present work, in order to verify the proper operation of the proposed autocalibration procedure and its applicability, we have developed, evaluated and validated disposable potentiometric test strips as demonstrators for the analysis of chloride ions in sweat which can be applied for cystic fibrosis (CF) diagnosis. This inherited disease causes severe damage to lungs, digestive tract, reproductive system and other organs in the body, and can be fatal. Its diagnosis in newborn screening tests allows patients maintaining a better life quality and life expectancy [33]. High chloride ion concentration in sweat is often used as a confirmatory biomarker of the disease. Values fewer than 30 mM in newborns and 40 mM in the rest of the population are not pathological, while in case of concentrations between 30/40 and 60 mM respectively, additional tests are required to confirm the disease diagnostic. Concentrations above 60 mM are pathological in all cases [34].

It is expected that the novel autocalibration strategy presented can be applied, for the potentiometric determination of different parameters in liquid samples in multiple fields of application that require simplicity, ease of use, and portability but also precision and on-site analytical information, by changing the ISEs on the test strip and after an optimization stage. Biomedicine (hospital or home point-of-care follow-up), environmental analysis and industrial processes and food control are a few examples of these fields of application.

2. Materials and methods

2.1. Materials and reagents

In order to fabricate the disposable potentiometric test strips prototypes, different substrate materials were used: a 50 μm-thick double faced pressure sensitive adhesive (PSA) tape (FAD 50 V, Flexcon, Spencer, USA) and two different types of COC layers (Tekni-Plex, Erembodegem, Belgium): 400 and 200 μm-thick COC 5013 sheets with a glass transition temperature (Tg) of 130 °C and 25 μm-thick COC 8007 foils with Tg of 75 °C. The electrodes (both indicator and reference) were fabricated using a Ag/AgCl (60/40) paste (C2130809D5, Sun Chemical Corporation, Bath, UK). A low gelling temperature (26–30 °C) agarose hydrogel (Sigma Aldrich, St Louis, USA) was used to imbibe and stabilize reagents on the electrodes.

All reagents used to carry out the analytical characterization and validation of the developed test strips and the autocalibration protocol were of ACS grade or similar from Merck-Sigma Aldrich, and Milli-Q water was used to prepare the corresponding solutions. Chloride standard solutions were obtained by serial dilutions from a 1 M NaCl stock solution. A 100 mM phosphate buffer adjusted to pH 5.5 (sweat pH) was used to keep buffered pH and ionic strength.

2.2. Fabrication of the disposable potentiometric test strips

The disposable potentiometric test strips were fabricated applying a multilayer microfabrication protocol partially described previously [35–37], consisting in a sequential hybrid process of thermal lamination and lamination at room temperature using COC layers and double faced PSA tapes. COC 8007 foils were used as heat sealing foils, PSA tapes were used as pressure adhesive layer and COC 5013 sheets were used as structural layers, where all patterns were micromachined. Six manufacturing steps were required: device design, structures micromachining, electrodes integration, thermal lamination, hydrogel deposition and final lamination at room temperature.

For the purpose of designing the structure of the test strips, computer-aided design (CAD) software was used. The layout has three main parts (Fig. 1A): the bottom layer (c) consists of a block of two previously laminated 400 μm-thick COC 5013 sheets (Tg = 130 °C) with a 25 μm-thick COC 8007 heat sealing foil (Tg = 75 °C) in between, which contains the Ag/AgCl electrodes; the middle layer (b) consists of a 200 μm-thick COC 5013 sheet with a previously thermolaminated sealing foil, patterned with the cavities (electrode and salt bridge) to be filled by hydrogel with the corresponding solutions; and the top layer (a) consists of a 200 μm-thick COC 5013 sheet with a 50 μm-thick PSA tape bonded,

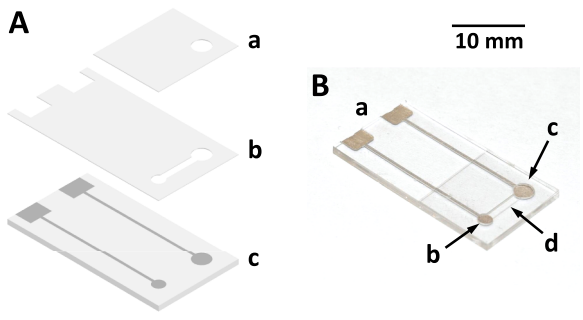

Fig. 1. A: Layered test strip design with top (a), middle (b) and bottom (c) layers. B: Image of the potentiometric disposable test strip where: a) Electric connectors; b) Reference electrode (ISE A); c) Indicator electrode (ISE B); d) Salt bridge.

which contains the sample chamber. Reference and indicator electrodes diameters are 1.8 mm and 2.6 mm, respectively. Salt bridge dimensions (L x W x H) are 5 mm x 1 mm x 0.23 mm. Volumes of each cavity on reference and indicator electrodes are 0.6 and 1.2 μL, respectively. Test strips dimensions (L x W x H) are 13 x 25 x 1.3 mm and weight is only 350 mg.

An automated computer controlled micromilling machine (Protomat C100/HF, LPKF, Germany), was used for COC layers micromachining.

A Ag/AgCl paste was used for the integration of the indicator and reference electrodes, by following a previously optimized protocol [15,38]. It consists of filling the different bas-reliefs machined on the COC layer with the conductive ink (Fig. 1Ac) and then curing it at 80 °C for 30 min. After that, layers b and c were thermally laminated using a temperature-controlled press (Francisco Camps, Granollers, Spain) set at 105 °C and 6 bar of pressure.

In order to confine reagents so that they remain stabilized in the corresponding chamber and to prevent chloride ion diffusion between electrodes during the sample measurement, a 2 % agarose hydrogel imbibed with different compositions was employed. Two types of agarose hydrogel solutions were employed: the first one, deposited on the indicator electrode and the salt bridge contained a phosphate buffer at pH 5.5 with 10 mM chloride concentration; and the second one, deposited on the reference electrode contained the same buffer but with a 100 mM chloride concentration. Both hydrogels were prepared by adding the necessary amount of agarose to a certain volume of the solution to imbibe and bringing the mixture to its certain melting temperature using a heating plate with magnetic stirring (Fisherbrand, USA). Once the agarose was melted, the resulting solution was deposited onto the corresponding chambers until they were filled. Four different types of agarose (Sigma Aldrich, Germany) with melting and gelling temperatures between 36 – 90 °C and 8 – 36 °C, respectively, were evaluated. By cooling to 8 – 36 °C, the solution gelled and the hydrogel formed. Finally, a lamination between block "b-c" (Fig. 1A), containing hydrogels, and block "a" was carried out at room temperature using the PSA tape and applying a pressure of 4 bar. The construction of the test strip was completed (Fig. 1B) and ready to be used immediately. The rapid preparation, deposition and encapsulation of the hydrogel solutions in the corresponding chambers allow avoiding the evaporation of water and thus the modification of chloride concentrations. To increase the prototype lifetime, the sample chamber can be sealed until the test strip use to prevent the evaporation of the solution contained in the hydrogel.

2.3. Experimental setup

The simple experimental setup used to carry out the potentiometric measurements is schematized in Fig. 2A. A customized miniaturized potentiometer (6017- COM16, TMI, Barcelona, Spain) was used for the acquisition and processing of the signals.

Sample chamber, where standard solutions or samples are added, is over the indicator electrode (see ISE B in Fig. 2), on the right side of the test strip. The reference electrode (see ISE A in Fig. 2) is in contact with a hydrogel solution with fixed chloride concentration providing a constant potential value.

To favor analyte diffusion from sample to the surface of the indicator electrode and thus shortening the analysis time, a customized eccentric rotating mass (ERM) actuator (similar to that used in mobile phones) working at a 180 Hz was used.

In order to simplify optimization process, calibration experiments in solution under batch conditions were performed. In this case, both electrodes from the test strip were evaluated as working electrodes and the electrochemical cell was completed by using a commercial reference electrode (Orion™ 900200). In this way, the dual electrode configuration or autocalibration protocol were not involved in the results obtained but allowed the evaluation of the electrodes performance.

2.4. Novel autocalibration procedure

The novel autocalibration process presented in this work is a very simple procedure that can be applied to potentiometric measurements in general. The only requirement is to use two ISEs selective for the same analyte and a specific composition of the hydrogels.

The process of autocalibration and sample measurement is shown in Fig. 2 with example data to understand data treatment.

As explained in section 2.2, each electrode is in contact with a hydrogel containing solutions with different but perfectly known analyte concentrations. These concentrations must be also higher than the concentration at the lower limit of the linear response of the ISEs. At the situation when the concentration difference between both solutions in contact with the electrodes is of a decade, the value of the measured potential (E) will be equal to the slope of the calibration equation but opposite sign. For instance, in the case of the studied application, concentrations in the hydrogels are 10 mM Cl^- (indicator electrode) and 100 mM Cl^- (reference electrode).

Calibration function follows Nernst equation that can be generalized

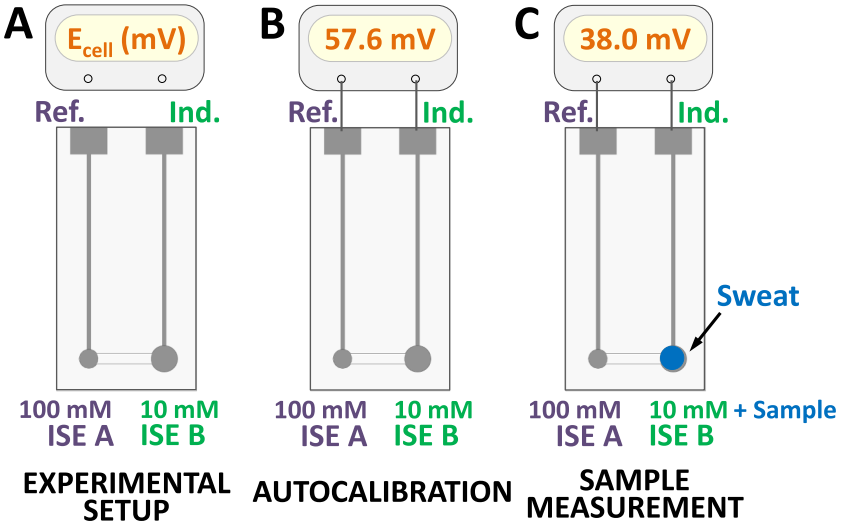

Fig. 2. Scheme of the autocalibration and sample measurement processes (drawing is not to scale). A) Initial step just before connecting the test strip to the potentiometer; B) Autocalibration step, when test strip is connected to the potentiometer and the calibration equation is automatically obtained; C) Sample analysis step, when a drop of sample is added to the sample chamber on the indicator electrode. Ref.: reference electrode; Ind.: Indicator electrode.

as Eq. (1), where "a" is the y-intercept and "b" the slope or sensitivity, and if an ionic strength similar to the one expected in the samples is set, the activity coefficient will be constant and then concentrations ($[Cl^-]$) can be used instead of activities (a_{Cl^-}). Although the theoretical value of the slope should be 59.16 mV for monovalent ions, the actual value will differ slightly depending on the characteristics of the electrode and the experimental conditions used. This uncertainty associated with the coefficients of the Nernst equation is the reason to perform the autocalibration procedure. Taking into account that the measured cell potential (E_{cell}) is the difference between the potential of the half-cell acting as indicator and the one acting as reference (Eq. (2)), assuming that the coefficients of the Nernst expressions on each half-cell are the same because both electrodes are the same, and knowing the concentrations of the analyte in the chamber of each half-cell (10 mM and 100 mM), we can obtain the slope of the potentiometric test strip (Eq. (3)) as the measured potential once the test strip is connected to the potentiometer (Fig. 2B) but opposite sign (for this example is $E_{autocalibration} = 57.6$). Rearranging equations and taking into consideration that the potential of the reference half-cell (E_{ref}) is constant, the cell potential depends solely on the potential of the half-cell of the indicator electrode. Thus, the calibration equation (Eq. (4)) of the test strip is obtained automatically at this precise moment of the test strip connection to the potentiometer, and it is then ready for sample analysis.

$$E = a + b\cdot\log(a_{Cl^-}) = a + b\cdot\log[Cl^-] \quad (1)$$

$$E_{autocalibration} = E_{ind} - E_{ref} = a + b\cdot\log[Cl^-]_{ind} - (a + b\cdot\log[Cl^-]_{ref}) \quad (2)$$

$$E_{autocalibration} = 57.6\,mV = b\cdot\log\left(\frac{10}{100}\right) \rightarrow b = -57.6\,mV\,dec^{-1} \quad (3)$$

$$E_{sample} = -57.6\log\left(\frac{[Cl^-]_{sample\ chamber}}{100}\right) = 38\,mV \rightarrow [Cl^-]_{sample\ chamber} = 22\,mM \quad (4)$$

$$[Cl^-]_{sample\ chamber} = \frac{V_{chamber}\cdot[Cl^-]_{initial} + V_{sample}\cdot[Cl^-]_{sample}}{(V_{chamber} + V_{sample})} \rightarrow [Cl^-]_{sample} = 34\,mM \quad (5)$$

To proceed with the measurement, a known volume of the sample is added into the sample chamber on the indicator electrode (Fig. 2C), and after a stabilization time, a potential value (E_{sample}) can be read, which for this example is 38 mV (Eq. (4)). By interpolation into the previously obtained calibration expression and taking into account a) the known volume ratio between the sample chamber and the added sample (in this example both are the same to facilitate calculations), and b) the $[Cl^-]$ in the hydrogel before the addition of the sample; finally the concentration of Cl^- in the sample is obtained with Eq. (5). Note that in order to obtain more accurate results, activities can be used instead of concentrations.

2.5. Sweat samples preparation

Two different types of samples were used to validate the autocalibration concept: synthetic samples and human sweat. Synthetic samples were prepared taking into account the average expected concentration of the main components found in human sweat according to bibliography [39]. Thus, 5 samples were prepared with a matrix of 50 mM sodium, 5 mM potassium, 22 mM lactate, 8 mM urea, 16 mM ethanol, 3 mM bicarbonate, 5 mM ammonia and 0.1 mM glucose and increasing concentrations of 10, 30, 50, 100 and 150 mM Cl^- (covering the desired chloride working range).

As for sweat samples, the gold standard for diagnosing CF (known as sweat test) establishes a very strict sampling protocol so that results on chloride determination are representative, allowing a reliable diagnosis of the disease [34,40]. Taking into account that the final objective of the present work is only the validation of the results provided by the developed test strips compared with a reference method, sweat sampling protocol was modified. The sampling followed a simplified protocol, which consisted on collecting sweat generated by perspiration of volunteers caused by exposure to high ambient temperatures or prolonged physical exercise and its further storage in vials. Throughout this process sweat samples evaporates and therefore, higher analyte concentrations are found compared to sweat samples obtained with the appropriate protocol. Even so, these samples can be used for the validation of the test strip with autocalibration procedure in a real sweat matrix of unknown chloride concentration. 16 samples from different anonymous volunteers were analyzed. Ion chromatography (IC) was selected as the reference method for the determination of chloride in sweat samples. Dionex Integrion equipment with a Dionex AS-AP autosampler (Thermo Scientific, USA) was used. Samples were filtered before analysis with 0.22 μm pore size filters due to operational requirements of the comparison method.

3. Results and discussion

3.1. Design and optimization of the disposable potentiometric test strip

Different structural, chemical and operational variables were evaluated in the development of the disposable potentiometric test strips in order to guarantee the best results in terms of sensitivity, selectivity, precision, accuracy, linear range, analysis time, amount of sample, reagents and materials needed, and ease of use (Table 1).

First of all, the dimensions of the electrodes and the volume of the chambers containing the hydrogels were optimized (Fig. S1). It is well known that in potentiometry, where the current is practically zero, the area of the electrodes does not have any influence on the potential measured. Nevertheless, the aim was to find suitable dimensions to simplify the manufacturing process and also the deposition of hydrogels. In this way, two electrode dimensions (1.8 and 2.6 mm in diameter), thus two chamber volumes on the electrodes (0.6 and 1.2 μL) were evaluated. As expected, no significant differences were found between calibrations obtained with electrodes with different areas or different chamber volumes. However, dispensing with precision sub-microliter volumes of hydrogel is complex. In order to simplify the manufacturing process and bearing in mind that it is not essential to know precisely the solution volume on the reference chamber (this does not apply to the sample chamber), a volume of 0.6 and 1.2 μL of chamber on the reference and indicator electrodes were selected, respectively. The latter was chosen to match the sample volume (1.2 μL) and thus, simplify further calculations. This volume was dispensed by using a micropipette.

Another designing parameter to optimize was the length and shape of the salt bridge microchannel (that is, the separation between electrodes). The objective was to prevent chloride ions diffusion from the

Table 1
Optimization of design, chemical and operational variables.

Variable	Studied interval	Optimal value
Chamber volume on indicator electrode (μL)	0.6 – 1.2	1.2
Chamber volume on reference electrode (μL)	0.6 – 1.2	0.6
Sample Volume (μL)	0.6 – 1.2	1.2
Agarose hydrogel:		
Melting temperature (°C)	36 – 90	65
Gelling temperature (°C)	8 – 36	26
Buffer	Phosphate, Citrate, acetate	Phosphate
Buffer concentration (mM)	10 – 2000	100
Buffer pH	4 – 7	5.5
Analysis time (min)	1 – 10	5

chamber on the reference electrode (higher concentration) to the sample chamber on the indicator electrode (lower concentration) during the measurement time, thus preserving the quality of the results. Different lengths (between 4.5 and 18 mm) and shapes (straight line and meander configuration) were tested (Fig. S2). To monitor the diffusion process between chambers, hydroxyl ion (which has an ionic mobility almost 3 times higher than chloride ion) was used as model ion and added as a sample to the sample chamber over the indicator electrode. The hydrogel on the chambers of the indicator and reference electrodes and on the salt bridge microchannel contained, for this experiment, the acidochromic dye phenol red in its acidic form. The mobility of hydroxyl ion from one chamber to the other was visualized by a color change (from yellow to violet color). Thus different diffusion times between both chambers were calculated depending on the salt bridge microchannel configuration. The selected one consisted of a straight channel joining the two ISE chambers (reference and sample) with a length of 4.5 mm. This configuration is the simplest and avoids, during at least 20 min, the modification of the chloride concentration on the chambers of the electrodes due to diffusion phenomena.

In fact, the use of a hydrogel with a polymeric matrix nature aims to difficult the undesired ion diffusion processes between chambers during the measurement process. Agarose was selected, since its characteristics such as low cost, biocompatibility, non-toxicity and ease and speed of preparation were optimal to the desired application [41,42]. It was weighted and fully melted into the desired total volume of a specific solution composition (buffer and chloride ion). From the four different types of agarose tested (Table S1), the one with a melting and gelling temperature of 65 and 36 °C, was chosen, since it provided conditions of use that facilitate the devices manufacturing process. Regarding the percentage of polymer, 2 % was selected (0.5 to 3 % were evaluated) because it provided a suitable hydrogel consistency for the application studied.

Three possible buffer compositions using citrate, acetate or phosphate, were evaluated by performing calibration experiments under batch (Fig. S3), as explained in section 2.3. Regarding the buffer concentration and pH, these were evaluated between 10 and 2000 mM (Fig. S4) and pH 4 and 7 (Fig. S5). Similar analytical features were obtained, so the three buffer solutions could be used. For reasons of stability and cost of the reagents, phosphate buffer was selected. In order to keep the ionic strength high enough and constant, and pH at values similar to those of sweat (pH 5.5), the optimal selected values were a buffer concentration of 100 mM and a pH of 5.5.

Regarding the analysis time, different options between 1 and 10 min with and without enhancing mixing by vibration were evaluated. A time of 5 min with vibration aid was necessary to obtain adequate results in the entire desired range of chloride concentrations (10 – 150 mM).

Finally, the influence of potential interfering ions present in sweat on the indicator ISE was also evaluated in batch conditions. Sweat is a rather complex aqueous mixture of different chemical compounds. According to the literature, there are two anions that are present at high concentrations in sweat and that could potentially interfere with the response of ISEs. These are bicarbonate, which can be found between 0.5 and 5 mM, and lactate, which can be found between 5 and 40 mM. Selectivity coefficients ($\log K_{i,j}^{pot}$) were not calculated because the response of the electrodes was not Nernstian at the highest concentration level of both interfering ions, however no significant differences were observed between calibrations with the buffer solution and solutions composed by the same phosphate buffer solution and 5 mM bicarbonate or 40 mM lactate (Fig. S6). Therefore, we can conclude that there is no interfering effect of these compounds on the response of the ISEs in the desired chloride range (10–150 mM). Similarly happens with pH. The expected range in human sweat samples can be between 4.5 and 6, with 5.5 being the typical value. As previously shown (Fig. S5), different chloride calibrations in batch were carried out at pH values of 4, 5, 5.5, 6 and 7, obtaining %RSD of the mean slope and y-intercept of less than 5 % in both cases, thus demonstrating that pH values in the range 4–7 do not affect the measurement process.

3.2. Evaluation of the feasibility of the autocalibration concept

Autocalibration is supported as long as the pair of electrodes on a test strip (reference and indicator ISEs) have a similar —ideally the same— response to the analyte, so that potential differences between them must be zero or close to zero, even when they may not exhibit Nernstian behavior (slope different from −59.2 mV dec^{-1}). A simple way to evaluate differences and the consequent measurement error produced in applying the concept of autocalibration is to measure the ΔE in mV obtained between the pair of ISEs of each disposable potentiometric test strip for a given chloride concentration acting both as a indicator electrodes. The smaller the ΔE, the smaller the error in the determination of the analyte by applying autocalibration. To demonstrate the applicability of the autocalibration concept, 16 test strips (16 pairs of electrodes) were evaluated. The 32 electrodes were individually calibrated in batch using a commercial Ag/AgCl reference electrode, obtaining an average calibration curve of $E_{average}$ = -58 (±1) log a_{Cl^-} + 41 (±1); r^2 = 0.9994. As example, Fig. 3A shows calibration curves of a pair of ISEs under test on test strip 1 and the ΔE in mV calculated for each of the 5 concentrations measured in the calibration process (10, 30, 60, 100 and 150 mM Cl^-). This was done for every pair of electrodes of the 16 evaluated test strips. From the 5 values of ΔE calculated, an average ΔE of each pair of electrodes in each test strip was extracted. Fig. 3B represents this average ΔE and the % error involved in chloride determination. Data suggest that the ISEs pairs from each test strip operate with remarkable concordance. This is supported by an average ΔE of around 1 mV across all pairs, signifying a chloride determination error of under 4 %, which coincides with the intrinsic error of the potentiometric technique. These results strongly validate the feasibility of the autocalibration concept.

3.3. Analysis of synthetic and real sweat samples

Once the conceptual basis of the autocalibration procedure was verified, the chloride content of 5 synthetic sweat samples was determined in order to evaluate the accuracy and precision of the procedure with a controlled matrix (Table 2).

The analysis was carried out using different test strips per triplicate and following the procedure explained in section 2.4 “Novel autocalibration procedure”. Once the test strip was connected to the potentiometer and the parameters of the calibration equation were obtained by autocalibration, 1.2 μL of the corresponding synthetic sample was added in the sample chamber over the hydrogel on the indicator electrode. After 5 min, measured potential was taken and used for chloride concentration calculations. In order to calculate the difference between considering concentrations instead of activities, chloride concentration values were also obtained using activities in the Nernst calibration expression only for the analysis of synthetic samples. To do that, the actual activity coefficients in each chamber for the autocalibration process and a theoretical activity coefficient ($\gamma_{calculated}$ = 0.75) to obtain the final concentration value, were used. The theoretical activity coefficient was calculated taking into account the ionic strength from the buffer (100 mM phosphate), an average concentration of Cl^- of 45 mM (which is the value in the middle of the critical range to diagnose CF and where better accuracy on the results is needed), and the average concentration of the rest of the ionic components present in the human sweat matrix, listed in section 2.5 “Sweat samples preparation”. All activity coefficients for this comparison were calculated using the extended Debye–Hückel expression [43].

As mentioned in the introduction, for sweat chloride concentrations between 30 mM and 60 mM, the diagnosis of cystic fibrosis requires additional tests, while values below 30 mM are a negative diagnosis and values above 60 mM are a positive diagnosis. Therefore, to achieve a

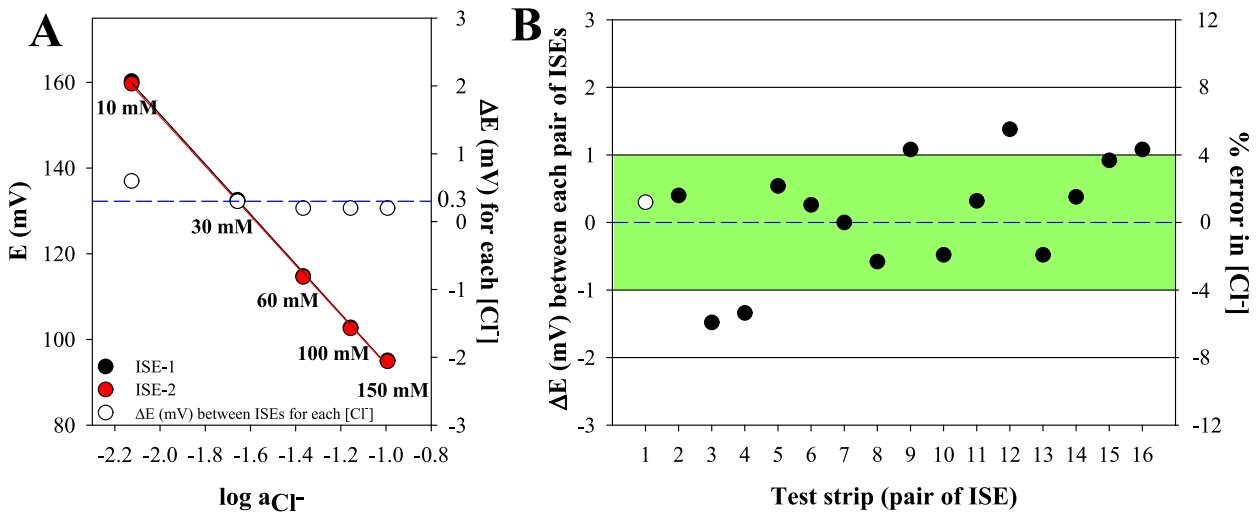

Fig. 3. A) Example of a calibration curve in batch between 10 and 150 mM Cl^- for a pair of ISEs in a test strip (strip 1) and representation of the ΔE in mV obtained for the pair of ISEs of the test strip 1 for each concentration and average value (0.3 mV in blue dashed line); **B)** Representation of the average ΔE in mV obtained from the calibrations of each pair of ISEs in batch and the percentage of error in the estimated chloride ion concentration for each test strip. In white the average AE (0.3 mV) calculated previously for test strip 1.

Table 2
Recovery studies with synthetic samples (n = 3; 95 % confidence).

Synthetic sweat sample	[Cl^-] added (mM)	[Cl^-] found directly (mM)	% recovery	[Cl^-] found from activities (mM)	% difference between [Cl^-] found
1	10	11 ± 1	112	12 ± 1	6
2	30	29 ± 2	98	30 ± 2	3
3	60	59 ± 3	98	59 ± 3	1
4	100	98 ± 2	98	98 ± 2	0
5	150	135 ± 4	90	135 ± 4	0

reliable diagnosis, it is necessary to obtain results as precise and accurate as possible around these concentrations. As we can observe from results, at the critical range of concentrations, we obtain recoveries very close to 100 %, with variations between the added value and the value directly found below 3 % and RSD for each value of concentration less than 3 %. Similarly, the difference between calculating concentration values directly and obtaining them through the use of activities is less than 3 % in the critical concentration range, with less difference at higher concentrations.

Therefore, in light of these results, we can conclude that the developed disposable potentiometric test strips and the mathematical approximations assumed in the autocalibration procedure, allow obtaining reliable results especially in the critical range of chloride concentrations.

Finally, 16 human sweat samples were analyzed in triplicate using different disposable potentiometric test strips and results, calculated directly as concentration using the procedure shown in section 2.4 "Novel autocalibration procedure", were compared with those obtained by ion chromatography. Results are shown in Table 3.

In general, the obtained chloride concentrations in real sweat samples are high as a result of the simplified sampling protocol followed, which increase chloride concentration due to sweat evaporation, but this fact has little relevance for this work, as previously stated. Accuracy of the proposed method is demonstrated since there are no significant differences between both methods, as shown in the paired *t*-test (t_{calc} = 0.445; t_{tab} = 2.131; $t_{calc} < t_{tab}$) and the linear regression (n = 16; 95 % confidence): $[Cl^-]_{IC}$ = 1.08 (± 0.08) $[Cl^-]_{POC}$ −6 (± 6); r^2: 0.981. In addition, confidence intervals achieved in general demonstrate the good precision of the measurements.

Results obtained demonstrate that the new autocalibration concept is

Table 3
Chloride ion concentrations (mM) using the different test strips (n = 3, 95 % confidence) and ion chromatography (IC) reference method.

Sample	Test strips (mM)	IC (mM)	% error
1	58 ± 0	51	13
2	102 ± 9	97	5
3	130 ± 7	135	−4
4	63 ± 4	62	2
5	56 ± 4	52	9
6	97 ± 8	100	−2
7	121 ± 2	138	−13
8	66 ± 6	61	8
9	103 ± 9	106	−3
10	58 ± 5	53	11
11	133 ± 9	144	−7
12	137 ± 15	133	3
13	88 ± 11	88	−1
14	10 ± 0	9	18
15	30 ± 4	31	−4
16	58 ± 2	61	−6

viable, successfully achieving the objectives of this work. However, certain aspects still need to be addressed to develop a market-ready product. First, an appropriate sample dosing system must be incorporated, similar to the one used in glucose test strips, where the sample volume required for analysis is precisely controlled by capillary action, filling a reservoir of known capacity. Additionally, to ensure long-term shelf life, a diffusion limiter must be used in the salt bridge to prevent the solutions on the electrodes from homogenizing. This could involve a physical barrier that dissolves at the time of measurement or a similar approach. These challenges will be addressed in future work to develop a prototype suitable for industrialization.

4. Conclusions

In the present work, a novel autocalibration procedure has been proposed to be applied to disposable potentiometric tests strips. Its application requires the use of devices integrating two identical ISEs. As a demonstrator, the concept has been successfully applied for the analysis of chloride ions in sweat.

The satisfactory results obtained in terms of precision, accuracy and reproducibility show that the proposed test strips configuration and the novel autocalibration concept have a very promising potential to be

employed to determine other parameters by mainly changing the used ISEs and the hydrogels composition.

With this innovative approach, the autocalibration of disposable potentiometric test strips without user intervention becomes feasible allowing its use for rapid and in-situ measurements out of laboratory environment.

Furthermore, the simplicity of the proposed potentiometric test strip makes it suitable for mass production, making it cost-effective and making it an ideal candidate for application as a disposable device.

Future work will be addressed to solve different technological issues related to the mass production of the test strips, reagent encapsulation, sampling, diffusion limiter in the salt bridge and the development of a portable potentiometer, similar to the glucose-meter concept. While the ultimate validation of the proposed innovation requires extending the test strip concept and autocalibration strategy to analyze other analytes in diverse sample matrices, the present work serves as a promising proof of concept, marking a significant stride in the field of disposable potentiometry.

CRediT authorship contribution statement

Antonio Calvo-López: Conceptualization, Data curation, Formal analysis, Investigation, Methodology, Software, Supervision, Validation, Writing – original draft. **Laia Garrido-Carretero:** Data curation, Formal analysis, Investigation, Software. **Julián Alonso-Chamarro:** Conceptualization, Funding acquisition, Project administration, Resources, Supervision, Writing – review & editing. **Mar Puyol:** Conceptualization, Funding acquisition, Project administration, Resources, Supervision, Writing – review & editing.

Declaration of competing interest

The authors declare that they have no known competing financial interests or personal relationships that could have appeared to influence the work reported in this paper.

Funding & Acknowledgments

The authors are grateful to Spanish Ministry of Science and Innovation and Catalan government for their financial support through the projects PID2020-117216RB-I00 and 2021SGR00124.

Appendix A. Supplementary data

Supplementary data to this article can be found online at https://doi.org/10.1016/j.jelechem.2024.118829.

Data availability

Data will be made available on request.

References

[1] M.I. Karayannis, C.E. Efstathiou, Significant steps in the evolution of analytical chemistry—Is the today's analytical chemistry only chemistry? Talanta 102 (2012) 7–15, https://doi.org/10.1016/j.talanta.2012.06.003.
[2] M. Valcárcel, Quo vadis, analytical chemistry? Anal. Bioanal. Chem. 408 (2016) 13–21, https://doi.org/10.1007/s00216-015-9148-6.
[3] A. Manz, H.M. Widmer, N. Graber, Miniaturized total chemical analysis systems: A novel concept for chemical sensing, Sensors Actuators B Chem. 1 (1990) 244–248, https://doi.org/10.1016/0925-4005(90)80209-I.
[4] A. Rios, A. Escarpa, B. Simonet, Miniaturization of the Entire Analytical Process II: Micro Total Analysis Systems (mTAS), in: Miniaturization Anal. Syst. Princ. Des. Appl., John Wiley & Sons, 2009: pp. 281–343.
[5] S. Jafari, J. Guercetti, A. Geballa-Koukoula, A.S. Tsagkaris, J.L.D. Nelis, M. P. Marco, J.P. Salvador, A. Gerssen, J. Hajslova, C. Elliott, K. Campbell, D. Migliorelli, L. Burr, S. Generelli, M.W.F. Nielen, S.J. Sturla, Assured point-of-need food safety screening: A critical assessment of portable food analyzers, Foods. 10 (2021), https://doi.org/10.3390/foods10061399.
[6] Y. Yang, Y. Chen, H. Tang, N. Zong, X. Jiang, Microfluidics for Biomedical Analysis, Small Methods 4 (2020) 1–30, https://doi.org/10.1002/smtd.201900451.
[7] A. Fernández-la-Villa, D.F. Pozo-Ayuso, M. Castaño-Álvarez, Microfluidics and electrochemistry: an emerging tandem for next-generation analytical microsystems, Curr. Opin. Electrochem. 15 (2019) 175–185, https://doi.org/10.1016/j.coelec.2019.05.014.
[8] S.A. Jaywant, K. Mahmood Arif, A comprehensive review of micro fluidic water quality monitoring sensors, Sensors (switzerland) 19 (2019), https://doi.org/10.3390/s19214781.
[9] M. Yew, Y. Ren, K.S. Koh, C. Sun, C. Snape, A Review of State-of-the-Art Microfluidic Technologies for Environmental Applications: Detection and Remediation, Glob. Challenges. 3 (2019) 1800060, https://doi.org/10.1002/gch2.201800060.
[10] S. Haeberle, R. Zengerle, Microfluidic platforms for lab-on-a-chip applications, Lab Chip. 7 (2007) 1094–1110, https://doi.org/10.1039/b706364b.
[11] D. Mark, S. Haeberle, G. Roth, F. Von Stetten, R. Zengerle, Microfluidic lab-on-a-chip platforms: Requirements, characteristics and applications, Chem. Soc. Rev. 39 (2010) 1153–1182, https://doi.org/10.1039/b820557b.
[12] X. Xu, S. Zhang, H. Chen, J. Kong, Integration of electrochemistry in micro-total analysis systems for biochemical assays: Recent developments, Talanta 80 (2009) 8–18, https://doi.org/10.1016/j.talanta.2009.06.039.
[13] A. Calvo-López, M. Puyol, J.M. Casalta, J. Alonso-Chamarro, Multi-parametric polymer-based potentiometric analytical microsystem for future manned space missions, Anal. Chim. Acta. 995 (2017) 77–84, https://doi.org/10.1016/j.aca.2017.08.043.
[14] A. Calvo-López, E. Martinez-Bassedas, M. Puyol, J. Alonso-Chamarro, Monitoring of total potassium in winemaking processes using a potentiometric analytical microsystem, Food Chem. 345 (2021), https://doi.org/10.1016/j.foodchem.2020.128779.
[15] A. Calvo-López, B. Rebollo-Calderon, A. Ormazábal, R. Artuch, J. Rosell-Ferrer, J. Alonso-Chamarro, M. Puyol, Biomedical point-of-care microanalyzer for potentiometric determination of ammonium ion in plasma and whole blood, Anal. Chim. Acta. 1205 (2022) 339782, https://doi.org/10.1016/j.aca.2022.339782.
[16] J. Hu, A. Stein, P. Bühlmann, Rational design of all-solid-state ion-selective electrodes and reference electrodes, TrAC - T, Trends Anal. Chem. 76 (2016) 102–114, https://doi.org/10.1016/j.trac.2015.11.004.
[17] N.L. Walker, A.B. Roshkolaeva, A.I. Chapoval, J.E. Dick, Recent advances in potentiometric biosensing, Curr. Opin. Electrochem. 28 (2021) 100735, https://doi.org/10.1016/j.coelec.2021.100735.
[18] R. Yan, S. Qiu, L. Tong, Y. Qian, Review of progresses on clinical applications of ion selective electrodes for electrolytic ion tests: from conventional ISEs to graphene-based ISEs, Chem. Speciat. Bioavailab. 28 (2016) 72–77, https://doi.org/10.1080/09542299.2016.1169560.
[19] V. Krikstolaityte, R. Ding, E. Chua Hui Xia, G. Lisak, Paper as sampling substrates and all-integrating platforms in potentiometric ion determination, TrAC - T, Trends Anal. Chem. 133 (2020) 116070, https://doi.org/10.1016/j.trac.2020.116070.
[20] F.X. Rius-Ruiz, G.A. Crespo, D. Bejarano-Nosas, P. Blondeau, J. Riu, F.X. Rius, Potentiometric strip cell based on carbon nanotubes as transducer layer: Toward low-cost decentralized measurements, Anal. Chem. 83 (2011) 8810–8815, https://doi.org/10.1021/ac202070r.
[21] J. Gonzalo-Ruiz, R. Mas, C. de Haro, E. Cabruja, R. Camero, M.A. Alonso-Lomillo, F.J. Muñoz, Early determination of cystic fibrosis by electrochemical chloride quantification in sweat, Biosens. Bioelectron. 24 (2009) 1788–1791, https://doi.org/10.1016/j.bios.2008.07.051.
[22] E. Zdrachek, T. Forrest, E. Bakker, Solid-Contact Potentiometric Cell with Symmetry, Anal. Chem. 94 (2022) 612–617, https://doi.org/10.1021/acs.analchem.1c04722.
[23] T. Forrest, T. Cherubini, S. Jeanneret, E. Zdrachek, P. Damala, E. Bakker, A submersible probe with in-line calibration and a symmetrical reference element for continuous direct nitrate concentration measurements, Environ. Sci. Process. Impacts. 25 (2022) 519–530, https://doi.org/10.1039/d2em00341d.
[24] C.R. Rousseau, P. Bühlmann, Calibration-free potentiometric sensing with solid-contact ion-selective electrodes, TrAC - Trends Anal. Chem. 140 (2021) 116277, https://doi.org/10.1016/j.trac.2021.116277.
[25] E. Bakker, Can Calibration-Free Sensors Be Realized? ACS Sensors 1 (2016) 838–841, https://doi.org/10.1021/acssensors.6b00247.
[26] Y.H. Cheong, L. Ge, G. Lisak, Highly reproducible solid contact ion selective electrodes: Emerging opportunities for potentiometry – A review, Anal. Chim. Acta. 1162 (2021) 338304, https://doi.org/10.1016/j.aca.2021.338304.
[27] J. Alonso Chamarro, M. Puyol Bosch, A. Calvo López, Disposable electrochemical sensing strips and associated methods, Patent, WO 2018/202635, 2018.
[28] P.S. Nunes, P.D. Ohlsson, O. Ordeig, J.P. Kutter, Cyclic olefin polymers: Emerging materials for lab-on-a-chip applications, Microfluid. Nanofluidics. 9 (2010) 145–161, https://doi.org/10.1007/s10404-010-0605-4.
[29] K.V. Guevara, P. Couceiro, H.C. Fuentes, A. Calvo-López, N. Sández, H.A. Moreno Casillas, F. Valdés Perezgasga, J. Alonso-chamarro, Microanalyser Prototype for On-Line Monitoring of Copper(II) Ion in Mining Industrial Processes, Sensors 19 (2019) 3382.
[30] N. Sández, A. Calvo-López, S.S.M.P. Vidigal, A.O.S.S. Rangel, J. Alonso-Chamarro, Automated analytical microsystem for the spectrophotometric monitoring of titratable acidity in white, rosé and red wines, Anal. Chim. Acta. 1091 (2019) 50–58, https://doi.org/10.1016/j.aca.2019.09.052.
[31] A. Calvo-López, O. Ymbern, M. Puyol, J. Alonso-Chamarro, Soluble reactive phosphorous determination in wastewater treatment plants by automatic microanalyzers, Talanta 221 (2021) 11–15, https://doi.org/10.1016/j.talanta.2020.121508.

[32] A. Agha, W. Waheed, N. Alamoodi, B. Mathew, F. Alnaimat, E. Abu-Nada, A. Abderrahmane, A. Alazzam, A Review of Cyclic Olefin Copolymer Applications in Microfluidics and Microdevices, Macromol. Mater. Eng. 307 (2022), https://doi.org/10.1002/mame.202200053.
[33] J.S. Elborn, Cystic fibrosis, Lancet 388 (2016) 2519–2531, https://doi.org/10.1016/S0140-6736(16)00576-6.
[34] P.M. Farrell, B.J. Rosenstein, T.B. White, F.J. Accurso, C. Castellani, G.R. Cutting, P.R. Durie, V.A. LeGrys, J. Massie, R.B. Parad, M.J. Rock, P.W. Campbell, Guidelines for Diagnosis of Cystic Fibrosis in Newborns through Older Adults: Cystic Fibrosis Foundation Consensus Report, J. Pediatr. 153 (2008), https://doi.org/10.1016/j.jpeds.2008.05.005.
[35] O. Ymbern, Development of centrifugal microfluidic platforms based on polymer microfabrication technology, Doctoral thesis, Universitat Autònoma De Barcelona (2015).
[36] A. Calvo López, Design, construction and evaluation of miniaturized analyzers for aerospace, environmental, food, biomedical and industrial applications, Doctoral thesis, Universitat Autònoma de Barcelona, 2017.
[37] O. Ymbern, M. Berenguel-Alonso, A. Calvo-López, S. Gómez-De Pedro, D. Izquierdo, J. Alonso-Chamarro, Versatile lock and key assembly for optical measurements with microfluidic platforms and cartridges, Anal. Chem. 87 (2015) 1503–1508, https://doi.org/10.1021/ac504255t.
[38] A. Calvo-López, E. Arasa-Puig, J. Alonso-Chamarro, M. Puyol, Serum/plasma potassium monitoring using potentiometric point-of-care microanalyzers with improved ion selective electrodes, Talanta 253 (2023), https://doi.org/10.1016/j.talanta.2022.124100.
[39] L.B. Baker, Physiology of sweat gland function: The roles of sweating and sweat composition in human health, Temperature. 6 (2019) 211–259, https://doi.org/10.1080/23328940.2019.1632145.
[40] V. LeGrys, R. Applequist, D. Briscoe, P. Farrell, R. Hickstein, S. Lo, R. Passarell, D. Rheinheimer, B. Rosenstein, J. Vaks, Clinical and Laboratory Standards Institute document C34-A3—Sweat Testing: Sample Collection and Quantitative Chloride Analysis, Approved Guideline—Third Edition, 2009.
[41] P.-E. Gustavsson, P.-O. Larsson, Chapter 6: Monolithic Polysaccharide Materials, in: Monolith. Mater. Prep. Prop. Appl., 2003: pp. 121–141.
[42] H.K. Mayer, G. Fiechter, Chapter, in: 10: Electrophoretic Techniques, 1st ed.,, 2013, https://doi.org/10.1016/B978-0-444-59562-1.00010-4.
[43] C.G. Patterson, D.D. Runnells, Geochemistry, Low-Temperature, in: Encycl. Phys. Sci. Technol., 2003: pp. 531–547. doi:10.1016/b0-12-227410-5/00191-5.